Inorg. Chem. **2006**, *45*, 8070–8077

CH···π Interaction for Rhenium-Based Rectangles: An Interaction That Is Rarely Designed into a Host–Guest Pair

Bala. Manimaran,[†,#] Liang-Jian Lai,[‡] P. Thanasekaran,[†] Jing-Yun Wu,[†] Rong-Tang Liao,[†] Tien-Wen Tseng,[‡] Yen-Hsiang Liu,[†] Gene-Hsiang Lee,[§] Shie-Ming Peng,[§] and Kuang-Lieh Lu*[,†]

Institute of Chemistry, Academia Sinica, Taipei 115, Taiwan, Department of Chemical Engineering, National Taipei University of Technology, Taipei 106, Taiwan, and Department of Chemistry, National Taiwan University, Taipei 107, Taiwan

Received March 20, 2006

Alkoxy- and thiolato-bridged Re^{I} molecular rectangles $[\{(CO)_3Re(\mu\text{-}ER)_2Re(CO)_3\}_2(\mu\text{-bpy})_2]$ (ER = SC_4H_9, **1a**; SC_8H_{17}, **1b**; OC_4H_9, **2a**; $OC_{12}H_{25}$, **2b**; bpy = 4,4′-bipyridine) exhibit strong interactions with several planar aromatic molecules. The nature of their binding was studied by spectral techniques and verified by X-ray diffraction analysis. Standard absorption and fluorescence titrations showed that a relatively strong 1:1 interaction occurs between aromatic guests such as pyrene and these rectangles. The results of a single-crystal X-ray diffraction analysis show that the recognition of **1** with a pyrene molecule is mainly due to CH···π interactions and the face of the guest pyrene is located over the edges of the bpy linkers of **1**. This is a fairly novel example of an interaction that is rarely designed into a host–guest pair. Furthermore, the interaction of **1** with Ag^+ results in the self-organization of supramolecular arrays, as revealed by solid-state data.

Introduction

Noncovalent interactions between host and guest molecules are ubiquitous in biology and include the vital functions of immune responses, transcription, replication, and biochemical signaling.[1−3] They also lie at the heart of several practical chemical technologies, including chemical sensing, separations, and catalysis.[4−6] Extensive efforts have been made to design components that mimic natural systems by undergoing molecular self-organization through selective noncovalent interactions such as H-bonding, electrostatic, and $\pi-\pi$-stacking interactions.[7−9] In addition, these noncovalent interactions have been actively used to strengthen structural and electronic communication between organic ligands in multifunctional metal complexes.[10] Among these, a CH···π interaction occurring between CH's (soft acids) and π groups (soft bases) has been noted as an important weak H-bond-

* To whom correspondence should be addressed. E-mail: lu@chem.sinica.edu.tw. Fax: int. code +886-2-27831237.
† Academia Sinica.
‡ National Taipei University of Technology.
§ National Taiwan University.
# Current address: Pondicherry University, India.

(1) (a) Samaranayake, M.; Bujnicki, J. M.; Carpenter, M.; Bhagwat, A. S. *Chem. Rev.* **2006**, *106*, 700. (b) Keeble, A. H.; Kirkpatrick, N.; Shimizu, S.; Kleanthous, C. *Biochemistry* **2006**, *45*, 3243. (c) Wang, T.; Gu, S.; Ronni, T.; Du, Y. C.; Chen, X. *J. Proteome Res.* **2005**, *4*, 941. (d) Dziadek, S.; Hobel, A.; Schmitt, E.; Kunz, H. *Angew. Chem., Int. Ed.* **2005**, *44*, 7630.

(2) (a) Graziewicz, M. A.; Longley, M. J.; Copeland, W. C. *Chem. Rev.* **2006**, *106*, 383. (b) Riguet, E.; Tripathi, S.; Chaubey, B.; Desire, J.; Pandey, V. N.; Decout, J. L. *J. Med. Chem.* **2004**, *47*, 4806. (c) Ren, J.; Qu, X.; Dattagupta, N.; Chaires, J. B. *J. Am. Chem. Soc.* **2001**, *123*, 6742.

(3) (a) Moro, S.; Gao, Z. G.; Jacobson, K. A.; Spalluto, G. *Med. Res. Rev.* **2006**, *26*, 131. (b) Zadmard, R.; Schrader, T. *J. Am. Chem. Soc.* **2005**, *127*, 904. (c) Shrout, A. L.; Montefusco, D. J.; Weis, R. M. *Biochemistry* **2003**, *42*, 13379.

(4) (a) Atwood, J. L.; Steed, J. W. *Supramolecular Chemistry*; John Wiley & Sons: Ltd.: Chichester, U.K., 2000. (b) Lehn, J. M. *Proc. Natl. Acad. Sci. U.S.A.* **2002**, *99*, 4763. (c) Hirschberg, J. H. K. K.; Brunsveld, L.; Ramzi, A.; Vekemans, J. A. J. M.; Sijbesma, R. P.; Meijer, E. W. *Nature* **2000**, *407*, 167. (d) Prins, L. J.; Reinhoudt, D. N.; Timmerman, P. *Angew. Chem., Int. Ed.* **2001**, *40*, 2382.

(5) (a) Lehn, J. M. In *The New Chemistry*; Hall, N., Ed.; Cambridge University Press: Cambridge, U.K., 2000; pp 200−251. (b) Davis, A. P.; Wareham, R. S. *Angew. Chem., Int. Ed.* **1999**, *38*, 2978. (c) Lee, H. K.; Park, K. M.; Jeon, Y. J.; Kim, D.; Oh, D. H.; Kim, H. S.; Park, C. K.; Kim, K. *J. Am. Chem. Soc.* **2005**, *127*, 5006.

(6) (a) Schug, K. A.; Lindner, W. *Chem. Rev.* **2005**, *105*, 67. (b) Atwood, J. L.; Barbour, L. J.; Dalgarno, S. J.; Hardie, M. J.; Raston, C. L.; Webb, H. R. *J. Am. Chem. Soc.* **2004**, *126*, 13170. (c) Meyer, E. A.; Castellano, R. K.; Diederich, F. *Angew. Chem., Int. Ed.* **2003**, *42*, 1210. (d) Przybylski, M.; Glocker, M. O. *Angew. Chem., Int. Ed. Engl.* **1996**, *35*, 806.

(7) (a) Yang, J.; Fan, E.; Geib, S. J.; Hamilton, A. D. *J. Am. Chem. Soc.* **1993**, *115*, 5314. (b) Lehn, J. M. *Pure Appl. Chem.* **1994**, *66*, 1961. (c) Timmerman, P.; Vreekamp, R. H.; Hulst, R.; Verboom, W.; Reinhoudt, D. N.; Rissanen, K.; Udachin, K. A.; Ripmeester, J. *Chem.—Eur. J.* **1997**, *3*, 1823. (d) Whitesides, G. M.; Simanek, E. E.; Mathias, J. P.; Seto, C. T.; Chin, D. N.; Mamen, M.; Gordon, D. M. *Acc. Chem. Res.* **1995**, *28*, 37. (e) Conn, M. M.; Rebek, J., Jr. *Chem. Rev.* **1997**, *97*, 1647.

(8) Whitesides, G. M.; Mathias, J. P.; Seto, C. P. *Science* **1991**, *254*, 1312.

(9) Percec, V.; Ahn, C.-H.; Ungar, G.; Yeardley, D. J. P.; Moller, M.; Sheiko, S. S. *Nature* **1998**, *391*, 161.

10.1021/ic0604720 CCC: $33.50
Published on Web 09/01/2006

Scheme 1. Molecular Rectangles **1** and **2**

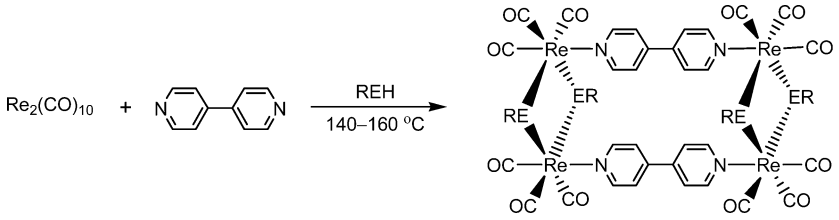

1a, E = S; R = $-(CH_2)_3CH_3$
1b, E = S; R = $-(CH_2)_7CH_3$
2a, E = O; R = $-(CH_2)_7CH_3$
2b, E = O; R = $-(CH_2)_{11}CH_3$

like force by many chemists and biochemists.[11] Despite being the weakest of the H bonds, it plays a significant role in tuning the physical, chemical, and biological properties of substances.[12−17] A number of calixarenes and cryptophans have been employed as potent synthetic macrocycles to include various guests, whereby CH···π interactions are believed to be a crucial driving force in determining the stability of host−guest complexes and in assembling molecular units into an organized supramolecular structure.[18−20] Hunter's group used an amide macrocycle with a highly preorganized cavity containing both polar and nonpolar recognition sites to form stable complexes with cyclic peptides in water via CH···π interactions.[21] During the investigation of organic conductive materials such as tetrathiafulvalene and related derivates, CH···π interactions were also reported to contribute significantly to the formation of two- and three-dimensional networks in addition to CH···S, $\pi-\pi$ stacking, and close chalcogen contacts.[22] CH···π interactions have also been inferred from structural studies of *p-tert*-butylcalix[4]arene·guest compounds, although some of these are significantly disordered.[23a,b] Kojima et al.[23c] have recently shown that the reaction of a Ru^{II} complex with β-diketone gave β-diketonato complexes in which hydrophobic $\pi-\pi$ or CH···π interactions were confirmed by NMR spectroscopy and X-ray crystallography. However, CH···π interactions in metallocyclophanes have been examined to a much lesser extent.[24] Herein we report on the characteristics associated with the recognition of thiolato- and alkoxy-bridged Re^{I} molecular rectangles with respect to several planar aromatic molecules and the Ag ion. Their recognition toward a highly conjugated aromatic guest, pyrene, via a perfect CH···π interaction was observed and confirmed by solid-state data. This is a fairly novel example of an interaction that is rarely designed into a host−guest pair. Furthermore, the interaction of the thiolato-bridged rectangle toward Ag ions results in the self-organization of an interesting supramolecular array.

Results and Discussion

Self-assembly and Characterization of Thiolato- and Alkoxy-Bridged Rectangles. The self-assembly of new thiolato-bridged Re^{I} molecular rectangles $[\{(CO)_3Re(\mu\text{-}SR)_2Re(CO)_3\}_2(\mu\text{-bpy})_2]$ (**1a**, R = C_4H_9; **1b**, R = C_8H_{17}) is achieved from $Re_2(CO)_{10}$, 4,4′-bipyridine (bpy), and mercaptan (butanethiol or octanethiol) under solvothermal conditions (Scheme 1). The known alkoxy-bridged molecular rectangles $[\{(CO)_3Re(\mu\text{-}OR)_2Re(CO)_3\}_2(\mu\text{-bpy})_2]$ (**2a**, R = C_8H_{17}; **2b**, R = $C_{12}H_{25}$) were prepared via literature procedures.[25] Preliminary studies of the thiolato- and alkoxy-

(10) (a) Coronado, E.; Galan-Mascaros, J. R.; Gomez-Garcıa, C. J.; Laukhln, V. *Nature* **2000**, *408*, 447. (b) Uji, S.; Shinagawa, H.; Terashima, T.; Yakabe, T.; Terai, Y.; Tokumoto, M.; Kobayashi, A.; Tanaka, H.; Kobayashi, H. *Nature* **2001**, *410*, 908. (c) Kitagawa, S.; Kitaura, R.; Noro, S. *Angew. Chem., Int. Ed.* **2004**, *43*, 2334 and references cited therein.
(11) (a) Mobian, P.; Kern, J. M.; Sauvage, J. P. *Angew. Chem., Int. Ed.* **2004**, *43*, 2392. (b) Schneider, H. J. *Angew. Chem., Int. Ed. Engl.* **1991**, *30*, 1417. (c) Su, C. Y.; Cai, Y. P.; Chen, C. L.; Smith, M. D.; Kaim, W.; zur Loye, H. C. *J. Am. Chem. Soc.* **2003**, *125*, 8595.
(12) (a) Nishio, M.; Hirota, M. *Tetrahedron* **1989**, *45*, 7201. (b) Nishio, M.; Umezawa, Y.; Hirota, M.; Takeuchi, Y. *Tetrahedron* **1995**, *51*, 8665. (c) Nishio, M.; Hirota, M.; Umezawa, Y. *The CH/π Interaction: Evidence, Nature and Consequences*; Wiley-VCH: Weinheim, Germany, 1998.
(13) (a) Miyake, Y.; Hosoda, A.; Takagaki, M.; Nomura, E.; Taniguchi, H. *Chem. Commun.* **2002**, 132. (b) Matsumoto, A.; Tanaka, T.; Tsubouchi, T.; Tashiro, K.; Saragai, S.; Nakamoto, S. *J. Am. Chem. Soc.* **2002**, *124*, 8891.
(14) (a) Matsumoto, A.; Sada, K.; Tashiro, K.; Miyata, M.; Tsubouchi, T.; Tanaka, T.; Odani, T.; Nagahama, S.; Tanaka, T.; Inoue, K.; Saragai, S.; Nakamoto, S. *Angew. Chem., Int. Ed.* **2002**, *41*, 2502. (b) Barreca, M. L.; Carotti, A.; Carrieri, A.; Chirri, A.; Monforte, A. M.; Calace, M. P.; Rao, A. *Bioorg. Med. Chem.* **1999**, *7*, 2283.
(15) (a) Amabilino, D. B.; Ashton, P. R.; Balzani, V.; Boyd, S. E.; Credi, A.; Lee, J. Y.; Menzer, S.; Stoddat, J. F.; Venturi, M.; Williams, D. J. *J. Am. Chem. Soc.* **1998**, *120*, 4295. (b) Vyas, N. K.; Vyas, M. N.; Quiocho, F. A. *Nature* **1987**, *327*, 635.
(16) (a) Matsugi, M.; Nojima, M.; Hagimoto, Y.; Kita, Y. *Tetrahedron Lett.* **2001**, *42*, 8039. (b) Kitamura, M.; Nakano, K.; Miki, T.; Okada, M.; Noyori, R. *J. Am. Chem. Soc.* **2001**, *123*, 8939.
(17) Quiocho, F. A.; Vyas, N. K. *Nature* **1984**, *310*, 381.
(18) (a) Notti, A.; Occhipinti, S.; Pappalardo, S.; Parisi, M. F.; Pisagatti, I.; White, A. J. P.; Williams, D. J. *J. Org. Chem.* **2002**, *67*, 7569. (b) Darbost, U.; Rager, M. N.; Petit, S.; Jabin, I.; Reinaud, O. *J. Am. Chem. Soc.* **2005**, *127*, 8517.
(19) (a) Canceill, J.; Lacombe, L.; Collet, A. *J. Am. Chem. Soc.* **1986**, *108*, 4230. (b) Canceill, J.; Cesario, M.; Collet, A.; Guilhem, J.; Lacombe, L.; Lozach, B.; Pascard, C. *Angew. Chem., Int. Ed. Engl.* **1989**, *28*, 1246.
(20) (a) Piatnitski, E. L.; Flowers, R. A., II; Deshayes, K. *Chem.—Eur. J.* **2000**, *6*, 999. (b) Arena, G.; Casnati, A.; Contino, A.; Lombardo, G. G.; Sciotto, D.; Ungaro, R. *Chem.—Eur. J.* **1999**, *5*, 738. (c) Oh, M.; Stern, C. L.; Mirkin, C. A. *Inorg. Chem.* **2005**, *44*, 2647.
(21) Allot, C.; Bernard, P. L.; Hunter, C. A.; Rotger, C.; Thomson, J. A. *Chem. Commun.* **1998**, 2449.
(22) (a) Potrzebowski, M. J.; Michalska, M.; Koziol, A. E.; Kazmierski, S.; Lis, T.; Pluskowski, J.; Ciesielki, W. *J. Org. Chem.* **1998**, *63*, 4209. (b) Nova, J. J.; Rovira, M. C.; Rovira, C.; Veciana, J.; Tarres, J. *Adv. Mater.* **1995**, *7*, 233.
(23) (a) Ungaro, R.; Pochini, A.; Andreetti, G. D.; Domiano, P. *J. Chem. Soc., Perkin Trans. 2* **1985**, 197. (b) Andreetti, G. D.; Pochini, A.; Ungaro, R. *J. Chem. Soc., Perkin Trans. 2* **1983**, 1773. (c) Kojima, T.; Miyazaki, S.; Hayashi, K. i.; Shimazaki, Y.; Tani, F.; Naruta, Y.; Matsuda, Y. *Chem.—Eur. J.* **2004**, *10*, 6402.
(24) (a) McNelis, B. J.; Nathan, L. C.; Clark, C. J. *J. Chem. Soc., Dalton Trans.* **1999**, 1831. (b) Boncella, J. M.; Cajigal, M. L.; Abboud, K. A. *Organometallics* **1996**, *15*, 1905.

bridged Re^{I}-based rectangles have been reported by Hupp et al.,[26] Sullivan et al.,[27] and Lu et al.[25] Compounds **1** and **2** are $M_4L_2L'_4$ types of neutral molecular rectangles that are self-assembled from 10 components. The solubility of the rectangles can be greatly improved by increasing the length of the alkyl chain present in the thiolato or alkoxy group. IR, NMR, and fast atom bombardment mass spectrometry (FAB-MS) spectra of the compounds and elemental analyses were all consistent with the proposed rectangular structures. Their architectures are further supported by single-crystal X-ray diffraction analyses (vide infra, Figures 1 and 8). Compounds **1** and **2** are neutral and air- and moisture-stable. Their electroneutrality, extensive solubility, and high stability make them potentially useful materials in sensor devices.

Interactions of 1 and 2 with Aromatic Hydrocarbons. Electronic absorption spectral measurements were carried out to investigate the ability of the rectangles to bind the highly conjugated aromatic guest pyrene. It is noteworthy that when pyrene is used as a probe and rectangles **1** and **2** are titrated in CH_2Cl_2, the absorbance of pyrene (guest) is enhanced with an increase in the concentration of the rectangular host, revealing a strong host−guest interaction between the rectangles and pyrene (Figure 2). The electron density of the Re^{I}-coordinated 4,4′-bpy ligand is reduced because of the metal coordination at the two pyridyl sites. Therefore, electron-rich pyrene is likely to form a charge-transfer (CT) complex with 4,4′-bpy of **1** and **2**, producing an adduct that is stabilized by donor−acceptor complexation. A new shoulder band observed at ∼360 nm is consistent with a CT absorption band.

The binding constants for the donor−acceptor complex formation between the rectangles and pyrene were evaluated using the Benesi−Hildebrand relationship (eq 1).[28]

$$1/\Delta A = 1/\Delta\epsilon[G] + (1 + \Delta\epsilon K[H][G]) \qquad (1)$$

Here ΔA is the change in the absorbance of the guest upon the addition of the host, $\Delta\epsilon$ denotes the difference in the molar extinction coefficient between the bound and free guest molecules, and K is the binding constant, while [H] and [G] are the total concentrations of the host and guest molecules, respectively. A double-reciprocal plot of the change in the intensity of the absorption of the guest with a change in the concentration of the host yields a linear correlation, indicating 1:1 host−guest complex formation. The binding constants (K) for this study are given in Table 1.

Further, the fluorescence intensities of pyrene in CH_2Cl_2 are efficiently quenched by rectangle **2a** in CH_2Cl_2. By an increase in the amount of **2a** added to the pyrene, the emission intensity of the latter decreases (Figure 3). The quenching is believed to be the result of an intermolecular transfer of energy from the emitting $\pi-\pi^*$ state of the guest to the low-lying CT excited state, which returns to the ground state via radiationless decay. It has been reported by the Yip group that CT interactions are responsible for the complexation of Au rectangles[29] and cyclobis(paraquat-*p*-phenylene) ions,[30] with electron-rich aromatic guests. Another study by

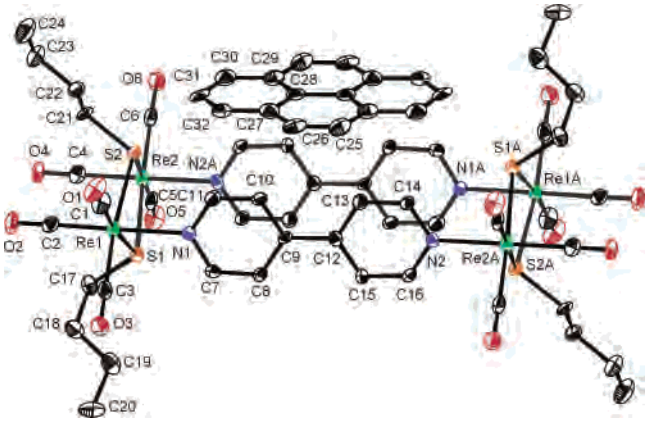

Figure 1. Crystallographic drawing of [**1a**·pyrene] showing CH···π interactions in the solid state.

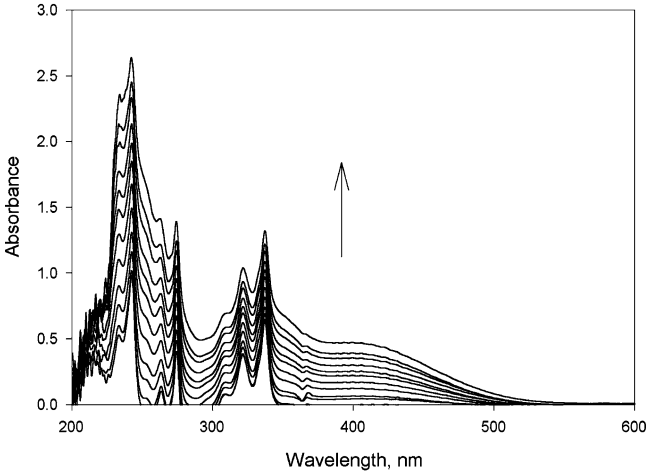

Figure 2. Electronic absorption spectra of pyrene (2×10^{-5} M) increasing with an increase in the concentration of host **2a** in dichloromethane: (a) 0 $\times 10^{-6}$, (b) 2×10^{-6}, (c) 4×10^{-6}, (d) 6×10^{-6}, (e) 8×10^{-6}, (f) 10×10^{-6}, (g) 12×10^{-6}, (h) 14×10^{-6}, (i) 16×10^{-6}, (j) 18×10^{-6}, (k) 20×10^{-6}, and (l) 22×10^{-6} M.

Table 1. Ground-State Binding Constants (K), Excited-State Dynamic (K_D) and Static (K_S) Stern−Volmer Constants, and Quenching Rate Constants (k_q) of Hosts **1** and **2** with Pyrene at 298 K

host	K, M^{-1}	K_D, M^{-1}	K_S, M^{-1}	k_q, $M^{-1}\ s^{-1}$
1a	1.9×10^4	7.4×10^4	3.6×10^4	2.3×10^{12}
1b	2.3×10^4	1.2×10^5	5.1×10^4	3.2×10^{12}
2a	9.7×10^3	3.5×10^4	1.7×10^4	1.1×10^{12}
2b	1.1×10^4	4.8×10^4	1.9×10^4	1.5×10^{12}

(25) (a) Manimaran, B.; Rajendran, T.; Lu, Y. L.; Lee, G. H.; Peng, S. M.; Lu, K. L. *J. Chem. Soc., Dalton Trans.* **2001**, 515. (b) Manimaran, B.; Thanasekaran, P.; Rajendran, T.; Lin, R. J.; Chang, I. J.; Lee, G. H.; Peng, S. M.; Rajagopal, S.; Lu, K. L. *Inorg. Chem.* **2002**, *41*, 5323.
(26) Benkstein, K. D.; Hupp, J. T.; Stern, C. L. *Inorg. Chem.* **1998**, *37*, 5404.
(27) Woessner, S. M.; Helms, J. B.; Shen, Y.; Sullivan, B. P. *Inorg. Chem.* **1998**, *37*, 5406.
(28) (a) Murakami, Y.; Kikuchi, J. I.; Suzuki, M.; Matsuura, T. *J. Chem. Soc., Perkin Trans. 1* **1988**, 1289. (b) Benesi, H. A.; Hildebrand, J. H. *J. Am. Chem. Soc.* **1949**, *71*, 2703.
(29) Lin, R.; Yip, J. H. K.; Zhang, K.; Koh, L. L.; Wong, K. Y.; Ho, K. P. *J. Am. Chem. Soc.* **2004**, *126*, 15852.
(30) (a) Nielsen, M. B.; Jeppesen, J. O.; Lau, J.; Lomholt, C.; Damgaard, D.; Jacobsen, J. P.; Becher, J.; Stoddart, J. F. *J. Org. Chem.* **2001**, *66*, 3559. (b) Ballardini, R.; Balzani, V.; Dehaen, W.; Dell'Erba, A. E.; Raymo, F. M.; Stoddart, J. F.; Venturi, M. *Eur. J. Org. Chem.* **2000**, 591.

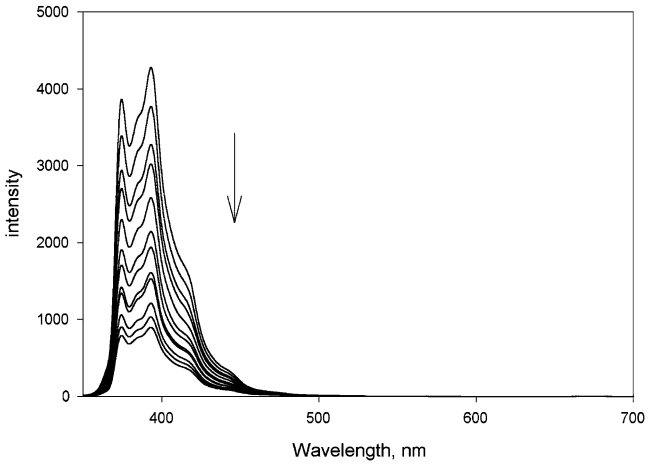

Figure 3. Emission intensity of pyrene (2×10^{-5} M) decreasing with an increase of the concentration of host **2a** in dichloromethane: (a) 0×10^{-6}, (b) 2×10^{-6}, (c) 4×10^{-6}, (d) 6×10^{-6}, (e) 8×10^{-6}, (f) 10×10^{-6}, (g) 12×10^{-6}, (h) 14×10^{-6}, (i) 16×10^{-6}, (j) 18×10^{-6}, (k) 20×10^{-6}, and (l) 22×10^{-6} M.

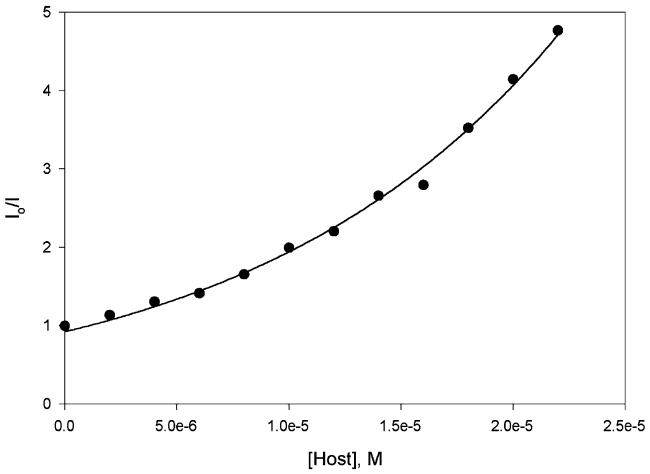

Figure 4. Stern−Volmer plot for the emission quenching of pyrene with an increase in the concentration of host **2a**.

Hupp and co-workers reported that the N-heterocyclic-bridged Re^{I} rectangles recognize guest molecules via electrostatic interactions or exterior side or intermolecular cavities.[31] Takagi and co-workers reported that the main contributions to CH···π interactions were the electrostatic and CT terms, based on an energy decomposition analysis.[32] Because both **2a** and pyrene are neutral species, we conclude that CT was observed as a result of the CH···π interaction.

The quenching rate constants, k_q, calculated from the Stern−Volmer equation are given in Table 1. The quadratic relationship between I_0/I and [Q] predicted an upward curvature in the Stern−Volmer plot.[33] This indicates that binding takes place along with efficient quenching. To explain the nonlinearity of the curve, the extended Stern−Volmer equation (eq 2) was used.

$$I_0/I = (1 + K_D[\text{host}])(1 + K_S[\text{host}]) \qquad (2)$$

where K_D and K_S are the dynamic and static Stern−Volmer constants, respectively. A nonlinear plot of eq 2 suggests the presence of a static component in the quenching mechanism along with dynamic quenching (Figure 4).

The values of K_D and K_S calculated from least-squares fitting are given in Table 1. Both the static (K_S) and dynamic (K_D) quenching rate constants were found, and a good agreement between binding constants (K) (obtained from absorption measurement) and K_S (obtained from emission measurement) was found. Complexation studies reveal that there is no significant difference in binding constants when the alkyl chain lengths of **1** and **2** are varied. The close resemblance of the experimental data to the theoretical fits using both UV−vis and an emission method is supportive of a 1:1 complexation model. Further, the high value of the quenching rate constant, k_q, indicates efficient bimolecular quenching between the Re^{I} rectangles and pyrene, along with binding.[34] Thus, we conclude that the unusual Stern−Volmer plots obtained are caused by the formation of a ground-state complex between the probe and the host.

Table 2. Complexation-Induced Shift Values for H^2 and H^3 of bpy in Host **1a** by Interaction with Aromatic Guests and Inorganic Salts[a]

	host + guest (δ, ppm)		shift ($\Delta\delta$, ppm)	
guest	H^3	H^2	H^3	H^2
diphenyl	9.073	7.795	−0.020	−0.060
pyrene	9.009	7.618	−0.084	−0.237
anthracene	9.072	7.801	−0.021	−0.054
triphenylene	9.042	7.741	−0.051	−0.114
benzopyrene	9.045	7.723	−0.048	−0.132
$AgNO_3$	9.356	7.859	+0.263	+0.004

[a] For free host **1a**, δ 9.093 and 7.855 ppm for H^3 and H^2 of bpy, respectively; [H] = [G] = 4×10^{-2} M.

The host−guest interaction of rectangle **1a** with aromatic hydrocarbons was investigated by monitoring the chemical shifts of δ_H of **1a** as a function of the different concentrations of the guest in acetone-d_6. The ^{1}H NMR studies showed that all of the guest protons and the H^3 and H^2 of the bpy of **1a** are shifted upfield. Similar upfield shifts have been observed in the binding of aromatic guests to the Pd cage[35] and a Au rectangle.[29] The H^2 signal of bpy is affected more than that of H^3 in all cases (Table 2), indicating that H^2 is more shielded by the π ring of the guests. Furthermore, there was only one set of signals for the entire titration, and the chemical shift of these signals changed as a function of the amount of guest added, suggesting that the exchange of the guest with **1a** is fast on the NMR time scale. Note that the alkyl protons of the alkoxy/thiolate bridges do not experience an appreciable change in the chemical shift upon the addition of the guests. These observations indicate that the added

(31) (a) Benkstein, K. D.; Hupp, J. T.; Stern, C. L. *J. Am. Chem. Soc.* **1998**, *120*, 12982. (b) Benkstein, K. D.; Stern, C. L.; Splan, K. E.; Johnson, R. C.; Walters, K. A.; Vanhelmont, F. W. M.; Hupp, J. T. *Eur. J. Inorg. Chem.* **2002**, 2818. (c) Benkstein, K. D.; Hupp, J. T.; Stern, C. L. *Angew. Chem., Int. Ed.* **2000**, *39*, 2891.

(32) Takagi, T.; Tanaka, A.; Matsuo, S.; Maezaki, H.; Tani, M.; Fujiwara, H.; Sasaki, Y. *J. Chem. Soc., Perkin Trans. 2* **1987**, 1015.

(33) (a) Wang, D.; Wang, J.; Moses, D.; Bazan, G. C.; Heeger, A. J. *Langmuir* **2001**, *17*, 1262. (b) Harrison, B. S.; Ramey, M. B.; Reynolds, J. R.; Schanze, K. S. *J. Am. Chem. Soc.* **2000**, *122*, 8561.

(34) (a) Sun, S. S.; Anspach, J. A.; Lees, A. J.; Zavalij, P. Y. *Organometallics* **2002**, *21*, 685. (b) Flamigni, L.; Johnston, M. R. *New J. Chem.* **2001**, *25*, 1368.

(35) Yoshizawa, M.; Nakagawa, J.; Kumazawa, K.; Nagao, M.; Kawano, M.; Ozeki, T.; Fujita, M. *Angew. Chem., Int. Ed.* **2005**, *44*, 1810.

Table 3. Crystal Data and Structure Refinement for [{**1a**·pyrene}·4C_3H_6O] and [{**1a**·$(Ag^+)_2(NO_3^-)_2(C_3H_6O)_2$}·$C_3H_6O$]

formula	$C_{76}H_{86}N_4O_{16}Re_4S_4$	$C_{60}H_{76}Ag_2N_6O_{22}Re_4S_4$
M_r	2184.53	2322.05
cryst syst	monoclinic	monoclinic
space group	$P2_1/c$	$P2_1/c$
a (Å)	10.4003(3)	11.7531(1)
b (Å)	22.2940(6)	18.0464(2)
c (Å)	17.3708(5)	18.7263(2)
β (deg)	99.082(2)	106.5641(5)
V (Å^3)	3977.2(2)	3807.04(7)
Z	2	2
D_{calc} (g cm^{-3})	1.824	2.026
μ(Mo Kα) (mm^{-1})	6.238	7.020
T (K)	120(1)	150(1)
cryst dimens (mm)	0.10 × 0.10 × 0.15	0.05 × 0.12 × 0.20
θ_{min}, θ_{max} (deg)	1.50, 27.50	1.60, 27.50
F(000)	2124	2224
reflns collected	29715	29301
indep reflns	8926 (R_{int} = 0.054)	8747 (R_{int} = 0.063)
observed data [$I > 2\sigma(I)$]	7305	6903
R1[a] [$I > 2\sigma(I)$]	0.0610	0.0396
wR2[a] [all data]	0.1518	0.1176
largest diff. peak, hole (e Å^{-3})	−2.43, 2.01	−2.07, 2.38
GOF	1.198	1.123

[a] R1 = $\sum||F_o| - |F_c||/\sum|F_o|$; wR2 = $[\sum w(F_o^2 - F_c^2)^2/\sum w(F_o^2)^2]^{1/2}$.

Table 4. Selected Bond Lengths (Å) and Angles (deg) of [{**1a**·pyrene}·4C_3H_6O]

Re1−S1	2.500(3)	Re1−S2	2.507(3)
Re1−N1	2.223(9)	Re1−C1	1.944(14)
Re1−C2	1.897(13)	Re1−C3	1.924(13)
Re2−S1	2.499(3)	C15−C16	1.384(17)
Re2−S2	2.497(3)	C17−C18	1.488(19)
Re2−C4	1.926(13)	C18−C19	1.47(2)
Re2−C5	1.859(14)	C19−C20	1.54(2)
Re2−C6	1.912(12)	Re2−N2a	2.217(9)
S1−C17	1.831(14)	S2−C21	1.830(11)
S1−Re1−S2	80.6(10)	N2a−Re2−C5	92.3(4)
S1−Re1−C1	173.2(5)	Re1−S1−Re2	98.49(11)
S1−Re1−C2	93.9(4)	Re1−S1−C17	111.3(4)
S1−Re1−C3	95.3(4)	Re2−S1−C17	106.3(4)
S2−Re1−C1	93.6(5)	Re1−S2−C21	111.6(4)
S2−Re1−C2	94.2(4)	Re2−S2−C21	105.2(4)
S2−Re1−C3	173.3(4)	Re1−N1−C7	121.2(7)
S1−Re2−C6	174.6(4)	Re2−C5−O5	175.1(10)
S2−Re2−C5	175.1(3)	S2−Re2−C6	95.1(4)

pyrene interacts strongly with the pyridyl protons of the bpy ligand of rectangle **1a**. This prompted us to further investigate the details of the interaction by a single-crystal X-ray diffraction analysis.

Solid-State Evidence of a Host−Guest Pair. To obtain insight into the host−guest binding mode, we attempted to obtain solid-state evidence for a **1a**·pyrene complex. Single crystals of [**1a**·pyrene] suitable for X-ray crystallographic analysis were obtained by the slow evaporation of solvent from an acetone solution of **1a** in the presence of pyrene at 25 °C. An ORTEP drawing of [**1a**·pyrene] is shown in Figure 1. The crystallographic refinement data and selected bond distances and angles are listed in Tables 3 and 4. The distances between Re1···Re2 and Re1···Re2A are 3.787 and 11.560 Å, respectively, confirming the rectangular architecture of **1a**. The two face-to-face bpy ligands in **1a** exhibit weak $\pi-\pi$-stacking interactions (both centroid···centroid distances are 3.730 Å), which significantly stabilize the structure of **1a**.

The crystallographic data unambiguously show that the pyrene binds to **1a** in a 1:1 ratio, consistent with observations from the Benesi−Hildebrand approach. The bpy ligands in **1a** interact with pyrene via CH···π interactions. The face of the pyrene guest sits over the edges of the bpy linkers, nearly orthogonal with a dihedral angle of approximately 95°. This is a fairly novel example of an interaction that is rarely designed into a host−guest pair. The central pyridyl H atoms (H10 and H13) interact with the π cloud of the pyrene with H(pyridyl)···C(pyrene) distances of 2.769−3.295 Å.

As shown in Figure 5, the host−guest pairs, **1a**·pyrene, are packed in a stairlike arrangement, in which the pyrene molecules are not located within the molecular cavity of **1a** but are parallel and remain in the space between the two different rectangle belts, leading to the formation of a supramolecular array. The spacing for accommodating the guest pyrene between the two parallel bpy linkers is ca. 6.40 Å, where the distances between the bpy C atoms in adjacent rectangles are 7.23−7.27 Å. This type of arrangement for CH···π interactions is perfect from the standpoint of the best overlap of the CH···π interactions (Figure 6).

Interaction of Thiolato-Bridged Rectangles with the Ag Ion. The Ag^I ion is regarded as an extremely soft acid, favoring coordination to soft bases, such as ligands containing S and unsaturated N.[36] Ag^I complexes with these soft ligands give rise to an interesting array of stereochemical and geometric configurations, with coordination numbers of 2−6 all occurring. In addition, Ag^I complexes with S-containing ligands have a wide range of applications in medicine, analytical chemistry, and the polymer industry.[37] The biomedical applications and uses of Ag^I complexes are related to their antibacterial action,[38] which appears to involve interactions with DNA.[39] Thus, the molecular design and structural characterization of Ag^I complexes are intriguing aspects of bioinorganic chemistry and metal-based drugs.[40] It has been established that, although thiolato groups coordinated to metal centers have the ability to bind to a second metal ion to form a S-bridged structure,[41,42] their binding ability toward higher oxidation state metal centers has recently been investigated.[43] We therefore examined the

(36) Suenga, Y.; Kuroda-Sowa, T.; Maekawa, M.; Munakata, M. *J. Chem. Soc., Dalton Trans*. **2000**, 3620 and references cited therein.
(37) (a) Krebs, B.; Hengel, G. *Angew. Chem., Int. Ed. Engl.* **1991**, *30*, 769. (b) Blower, P. G.; Dilworth, J. R. *Coord. Chem. Rev.* **1987**, *76*, 121. (c) Raper, E. S. *Coord. Chem. Rev.* **1996**, *153*, 199.
(38) Wruble, M. *J. Am. Pharm. Assoc. Sci. Ed*. **1943**, *32*, 80.
(39) Rosenkranz, H. S.; Rosenkranz, S. *Antimicrob. Agents Chemother.* **1972**, *2*, 373.
(40) (a) Nomiya, K.; Kondoh, Y.; Nagano, H.; Oda, M. *J. Chem. Soc., Chem. Commun*. **1995**, 1679. (b) Nomiya, K.; Takahashi, S.; Noguchi, R. *J. Chem. Soc., Dalton Trans.* **2000**, 2091.
(41) (a) Marr, A. C.; Spencer, D. J. E.; Schroder, M. *Coord. Chem. Rev.* **2001**, *219−221*, 1055. (b) Konno, T.; Chikamoto, Y.; Okamoto, K.; Yamaguchi, T.; Ito, T.; Hirotsu, M. *Angew. Chem., Int. Ed*. **2000**, *39*, 4098.
(42) (a) Blake, A. J.; Collison, D.; Gould, R. O.; Reid, G.; Schroder, M. *J. Chem. Soc., Dalton Trans.* **1993**, 521. (b) Clarkson, J.; Yagbasan, R.; Blower, P. J.; Rawle, S. C.; Cooper, S. R. *J. Chem. Soc., Chem. Commun*. **1987**, 950.
(43) Konno, T.; Shimazaki, Y.; Yamaguchi, T.; Ito, T.; Hirotsu, M. *Angew. Chem., Int. Ed.* **2002**, *41*, 4711.

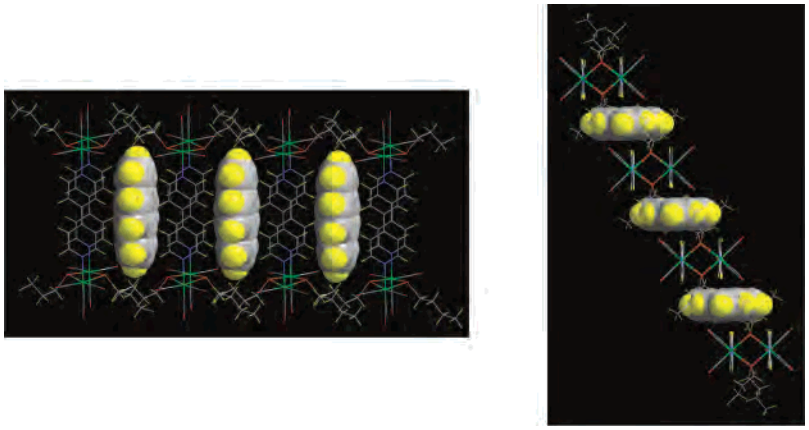

Figure 5. Crystal packing drawing of [{**1a**·pyrene}·4(acetone)] showing one-to-one host−guest interactions (left) and a stairlike arrangement (right) in the solid state.

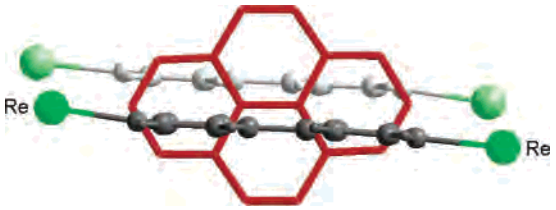

Figure 6. View of the CH···π interactions between the bpy ligands of host **1a** and the pyrene guest, showing the offset orientation between the two bpy ligands, which are placed above and below the pyrene molecule, respectively.

interaction of rectangles **1a** and **1b** with Ag^I because these rectangles contain thiolato bridges.

The electronic absorption spectrum of **1a** in 80:20 (v/v) THF−H_2O shows absorptions at 226, 243(sh), 322, and 384 nm. The high-energy absorption is assigned to a ligand-centered transition, and the low-energy values are assigned to metal-to-ligand CT transitions. Upon the addition of Ag^I to **1a**, a shift in the ligand-centered transition from 226 to 230 nm occurs with an increase in the absorbance. Meanwhile, during the addition of Ag^I, the shoulder at 243 nm disappears, but there is no appreciable change in the metal-to-ligand CT transition, the spectrum of which is shown in Figure 7. This implies that Ag^I ions affect only the $\pi-\pi^*$ transition of the bpy ligand in **1a**.

The lone pair electrons present on the S atom of the thiolato bridge of host **1** are proposed to coordinate to the Ag^I ion of $AgNO_3$. The IR spectrum of **1a** in the presence of the Ag^I ion in acetone shows a marked change in ν_{CO} absorption from 2018, 2005, and 1917 cm^{-1} to 2027, 2015, and 1914 cm^{-1}. Rectangles **1a** and **1b** that are capable of binding metal ions that undergo spectroscopic changes upon the formation metal ion complexes could be used as analytical reagents in the analysis of metal ions. ^1H NMR spectral studies of **1a** in the presence of the Ag^I ion in acetone-d_6 shows a downfield shift of the H^2 and H^3 protons of the pyridyl group (Table 2). This indicates the coordination of the Ag cation to the S atom, thus causing a reduction in the electron density on it and consequently on the metal. This, in turn, causes the Re atom to draw electrons from the bipyridyl moiety and, as a result, the H^2 and H^3 protons of the pyridyl group are shifted downfield. These observations

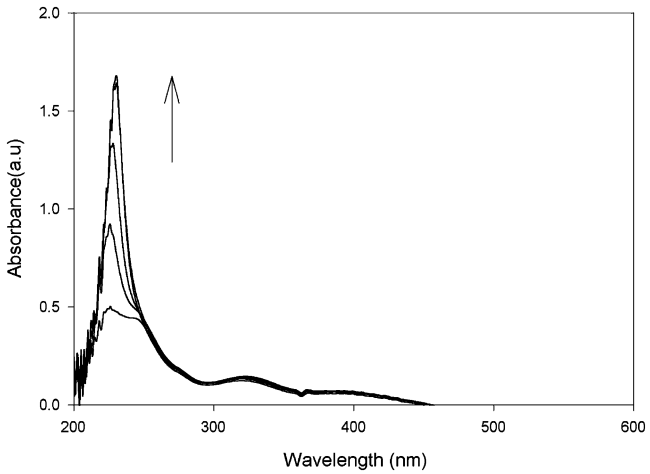

Figure 7. Absorption spectra of **1a** (1×10^{-5} M) upon the addition of the Ag^I ion in a 80:20 (v/v) THF−H_2O mixture: (a) 0, (b) 2×10^{-4}, (c) 4×10^{-4}, (d) 6×10^{-4}, and (e) 8×10^{-4} M.

indicate that the Ag^I···S interactions are significant. This is corroborated by the IR data. The marked change in ν_{CO} absorption to a higher wavenumber showed that back-bonding to the π^* orbital of CO is less because of the lower electron density at the Re center. The NO_3^-···H(bpy) interactions may occur but to a lesser extent than Ag^I···S interactions because nitrate anions (NO_3^-) may prefer to interact with Ag cations in solution (vide infra).[44]

To further verify these observations, X-ray-quality crystals of compound [{**1a**·$(Ag^+)_2(NO_3^-)_2(C_3H_6O)_2$}$(C_3H_6O)$] were obtained by dissolving the host **1a** with the guest $AgNO_3$ in acetone, followed by slow evaporation at room temperature. A single-crystal X-ray analysis reveals that the species contains one rectangle [{$(CO)_3Re(\mu\text{-}SC_4H_9)_2Re(CO)_3$}$_2(\mu\text{-}bpy)_2]_2$ unit, two Ag^I atoms, two bridging nitrate ions, and two coordinated acetone molecules. Complex [{**1a**·$(Ag^+)_2(NO_3^-)_2(C_3H_6O)_2$}$(C_3H_6O)$] crystallizes in a monoclinic cell, and the structure was solved in the space group $P2_1/c$. The crystallographic refinement data and selected bond distances and angles are listed in Tables 3 and 5. As shown in Figure 8, the thiolato bridges of the Re^I rectangles are coordinated

(44) Vega, I. E. D.; Gale, P. A.; Light, M. E.; Loeb, S. J. *Chem. Commun.* **2005**, 4913 and references cited therein.

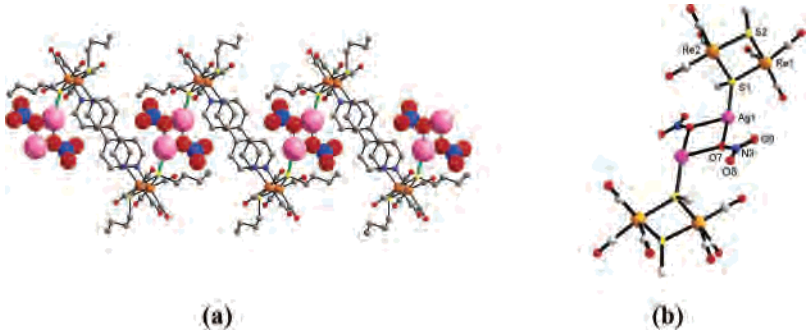

Figure 8. (a) Crystallographic drawing indicating the inclusion of $AgNO_3$ moieties by host **1a** through silver−thiolate side-arm interactions and formation of a linear supramolecular array. The coordinated acetone molecules are omitted for the sake of clarity. The $AgNO_3$ moieties are enlarged for clarity. (b) Details of the thiolate−silver−nitrate interactions. Key: orange, Re; yellow, S; pink, Ag; blue, N; red, O; gray, C.

Table 5. Selected Bond Lengths (Å) and Angles (deg) for $[\{\mathbf{1a}\cdot(Ag^{+})_2(NO_3^{-})_2(C_3H_6O)_2\}(C_3H_6O)]$

Re1−S1	2.5356(17)	Re1−S2	2.4964(16)
Re1−N1	2.213(5)	Re2−S1	2.5253(16)
Re2−S2	2.5135(17)	Re2−N2	2.230(5)
Re2−C4	1.926(7)	Re2−C5	1.924(7)
Re2−C6	1.919(7)	Ag1−S1	2.4405(17)
Ag1−O7	2.308(5)	Ag1−O10	2.432(5)
S1−C17	1.847(8)	S2−C21	1.837(7)
S1−Re1−S2	79.99(5)	S1−Re1−N1	88.82(14)
S1−Re1−C1	171.6(2)	S1−Ag1−O7	157.94(15)
S1−Re1−C2	90.8(2)	S1−Ag1−O10	119.49(13)
S1−Re1−C3	96.4(2)	S2−Re1−N1	85.37(14)
S2−Re1−C1	91.7(2)	S2−Re1−C2	94.8(2)
S2−Re1−C3	174.7(2)	Re1−S1−Re2	99.09(6)
Re1−S1−Ag1	126.79(7)	Re2−S1−Ag1	115.32(6)
Ag1−S1−C17	99.5(2)	Re1−S2−Re2	100.46(6)
S1−Re2−S2	79.87(5)	S1−Re2−N2	85.24(14)
S2−Re2−N2	88.00(14)		

to Ag atom [Ag1−S1, 2.4405(17) Å], which is further linked by two nitrate ions with the Ag−O distances of 2.308(5)−2.542(5) Å and coordinated by one acetone molecule [Ag1−O10, 2.432(5) Å; Supporting Information, Figure S6]. The intrinsic affinity of the S atom toward the Ag^{I} ion together with the $Ag-ONO_2$ interactions leads to the formation of a one-dimensional supramolecular array through S···Ag···O connections. Additionally, two adjacent Ag salts are bridged together through nitrate ions with Ag···Ag distances of about 4.05 Å. This reveals the existence of very weak argentophilic interactions in this system. Thus, the interaction of the rectangles toward the Ag ion results in the self-organization of interesting supramolecular arrays.

Conclusion

In summary, thiolato- and alkoxy-bridged molecular rectangles exhibit molecular recognition characteristics toward planar aromatic guest molecules and the Ag ion. As evidenced by UV−vis, fluorescence, and ^{1}H NMR spectroscopic data and single-crystal X-ray diffraction analyses, rectangles **1** and **2** strongly interact with the pyrene molecule in a 1:1 host−guest ratio. The results of a single-crystal X-ray diffraction analysis show that the recognition of **1** toward the pyrene molecule is mainly due to CH···π interactions and that the face of the guest pyrene sits over the edges of the bpy linkers of **1**. In addition, the thiolato-bridged rectangle **1a** recognizes Ag^{I}, generating an interesting supramolecular array via Re−S···Ag···O interactions.

Experimental Section

Materials and General Methods. Reagents were used as received without further purification. The solvents used in this study were of spectroscopic grade. Electronic absorption spectra were recorded on a Hewlett-Packard 8453 spectrophotometer. Fluorescence spectra were recorded on a Hitachi F4500 spectrometer using a slit width of 2.5 nm for both excitation and emission measurements. The photomultiplier voltage was 700 V. ^{1}H and ^{13}C NMR spectra were recorded on Bruker AC 300 and AMX-400 FT-NMR spectrometers. Elemental analyses were performed using a Perkin-Elmer 2400 CHN elemental analyzer. FAB-MS data were obtained using a JMS-700 double-focusing mass spectrometer.

Synthesis of $[\{(CO)_3Re(\mu\text{-}SC_4H_9)_2Re(CO)_3\}_2(\mu\text{-bpy})_2]$ (1a). A suspension containing a mixture of $Re_2(CO)_{10}$ (131 mg, 0.20 mmol) and bpy (65 mg, 0.40 mmol) in 10 mL of a 3:7 mixture of 1-butanethiol and toluene in a 30-mL Teflon flask was placed in an oven at 140 °C for 48 h and then cooled to 25 °C. The resulting orange crystals were separated by filtration, and the solvent from the filtrate was removed by applying a vacuum. The residue was redissolved in a minimum quantity of CH_2Cl_2 and passed through a short silica gel column to give the pure product. Yield: 71%. IR (CH_3COCH_3): ν_{CO} 2018 (s), 2005 (s), 1917 (vs), 1899 (vs) cm^{-1}. ^{1}H NMR (300 MHz, acetone-d_6): δ 9.09 (d, ^3J = 5.3 Hz, 8H, H^3), 7.86 (d, 8H, H^2), 3.32 (t, ^3J = 7.4 Hz, 8H, CH_2), 1.71 (m, 8H, CH_2), 1.57 (m, 8H, CH_2), 1.03 (t, ^3J = 7.2 Hz, 12H, CH_3). ^{13}C NMR (75 MHz, acetone-d_6): δ 201.0, 196.1 (1:2 CO), 157.0 (C^3), 145.5 (C^1), 123.6 (C^2), 39.5 (CH_2), 35.6 (CH_2), 22.3 (CH_2), 14.0 (CH_3). UV−vis (CH_3CN): λ_{max} [nm] 365 (MLCT), 244, 316 (LIG). FAB-MS: m/z 1750.2 (M^+). Anal. Calcd for $C_{48}H_{52}N_4O_{12}S_4Re_4$: C, 32.94; H, 2.99; N, 3.20. Found: C, 32.94; H, 2.82; N, 2.92.

Synthesis of $[\{(CO)_3Re(\mu\text{-}SC_8H_{17})_2Re(CO)_3\}_2(\mu\text{-bpy})_2]$ (1b). A suspension consisting of a mixture of $Re_2(CO)_{10}$ (98 mg, 0.15 mmol) and bpy (32 mg, 0.10 mmol) in 10 mL of a 3:7 mixture of 1-octanethiol and toluene in a 30-mL Teflon flask was placed in a steel bomb. The bomb was placed in an oven maintained at 140 °C for 48 h and then cooled to 25 °C. Good-quality orange single crystals of **1b** were obtained. The solvent from the reaction mixture was removed by vacuum distillation, and the residue was redissolved in CH_2Cl_2 and passed through a short silica gel column to get pure **1b**. Yield: 53%. IR (CH_2Cl_2): ν_{CO} 2019 (s), 2006 (s), 1919 (vs), 1898 (vs) cm^{-1}. ^{1}H NMR (300 MHz, acetone-d_6): δ 9.09 (d, ^3J = 6.7 Hz, 8H, H^3), 7.84 (d, ^3J = 6.7 Hz, 8H, H^2), 3.31 (t, ^3J = 7.3 Hz, 8H, CH_2), 1.76 (m, 8H, CH_2), 1.56 (m, 8H, CH_2), 1.41 (m, 16H, CH_2), 1.35 (m, 16H, CH_2), 0.91 (t, ^3J = 6.6 Hz, 12H, CH_3). ^{13}C NMR (75 MHz, acetone-d_6): δ 200.9, 196.1 (1:2 CO), 156.9 (C^3), 145.5 (C^1) 123.5 (C^2), 39.8 (CH_2), 33.6 (CH_2), 32.6 (CH_2), 29.9 (2CH_2), 23.3 (2CH_2), 14.4 (CH_3).

UV−vis (CH_3CN): λ_{max} [nm] 368 (MLCT), 244, 316 (LIG). FAB-MS: *m*/*z* 1974.2 (M^+). Anal. Calcd for $C_{64}H_{84}N_4O_{12}S_4Re_4$: C, 38.86; H, 4.28; N, 2.83. Found: C, 39.03; H, 3.74; N, 2.57.

Rectangles **2a** and **2b** were obtained following a similar procedure using 10 mL of aliphatic alcohol instead of a mixture of thiol and toluene.[25] Yield: **2a**, 86%; **2b**, 87%.

Fluorescence Quenching Studies. Quenching experiments of the fluorescence of pyrene were carried out under aerated conditions. The solvent used in this study was of spectroscopic grade. The excitation wavelength was 336 nm in CH_2Cl_2 as the solvent. The monitoring wavelength corresponded to the maximum of the emission band at 393 nm. Relative fluorescence intensities were measured for solutions of pyrene in CH_2Cl_2 and rectangles used as quenchers. There was no change in shape, but a change in the intensity of the fluorescence peak was found, when these rectangles were added. The Stern−Volmer (SV) relationship, $I_0/I = 1 + K_{SV}[Q]$, was obtained for the ratio of the emission intensities (I_0 and I are the emission intensities in the absence and presence of quencher) and quencher concentration, [Q]. The quenching rate constants were obtained from the Stern−Volmer constant, K_{SV}, and the fluorescence lifetime, τ, of pyrene (32 ns). Excited-state lifetime studies were performed using an Edinburgh FL 920 single photon-counting system with a H_2-filled or N_2 lamp as the excitation source. The emission decays were analyzed by the sum of exponential functions, which allows the partial elimination of instrument time broadening, thus rendering a temporal resolution.

Binding Constant Measurements. The binding abilities of the rectangles with pyrene were examined by both absorption and emission spectroscopic methods. The concentration of pyrene was 2×10^{-5} M, and those of the rectangles were 2×10^{-6}−3×10^{-5} M. The binding constants from the electronic absorption experiment were measured by changing the concentration of the rectangles with pyrene and calculated on the basis of the Benesi−Hildebrand relationship for a 1:1 molar ratio. A good linear correlation of $1/\Delta A$ vs 1/[H] was obtained for all of the measurements. The binding constants in the excited state were determined using the modified Stern−Volmer equation.

X-ray Crystallographic Studies. Suitable single crystals with dimensions of $0.10 \times 0.10 \times 0.15$ and $0.05 \times 0.12 \times 0.20$ mm for [{**1a**·pyrene}·$4C_3H_6O$] and [{**1a**·$(Ag^+)_2(NO_3^-)_2(C_3H_6O)_2$}·$(C_3H_6O)$], respectively, were selected for indexing and intensity data collection. A total of 1420 frames constituting a hemisphere of X-ray intensity data were collected with a frame width of 0.3° in ω and a counting time of 10 s/frame, using a Bruker SMART CCD diffractometer. The first 50 frames were re-collected at the end of data collection to monitor crystal decay. No significant decay was observed. The raw data frames were integrated into *SHELX*-format reflection files and corrected for Lorentz and polarization effects using the *SAINT* program, and absorption correction was performed using the *SADABS* program.[45] The space groups were determined to be $P2_1/c$. Direct methods were used to solve the structure using the *SHELX-TL*[46] program packages. All non-H atoms were refined anisotropically by full-matrix least squares based on F^2 values. The largest residual density peak is close to that of the Re atom. Basic information pertaining to crystal parameters and structure refinement for [{**1a**·pyrene}·$4C_3H_6O$] and [{**1a**·$(Ag^+)_2(NO_3^-)_2(C_3H_6O)_2$}$(C_3H_6O)$] is summarized in Table 3, and selected bond distances and angles are provided in Tables 4 and 5, respectively.

Acknowledgment. We thank Academia Sinica and the National Science Council, Taiwan, for financial support.

Supporting Information Available: Crystallographic details in CIF format, UV−vis absorption spectra of **2b** and pyrene, Stern−Volmer plot for **1a** with pyrene, and coordination environments around the Ag ions. This material is available free of charge via the Internet at http://pubs.acs.org.

IC0604720

(45) *SMART/SAINT/ASTRO*, release 4.03; Siemens Energy & Automation, Inc.: Madison, WI, 1995.
(46) Sheldrick, G. M. *SHELX-TL*; University of Gottingen: Gottingen, Germany, 1998.